Additive Manufacturing 16 (2017) 138–145

Contents lists available at ScienceDirect

Additive Manufacturing

journal homepage: www.elsevier.com/locate/addma

Full Length Article

Investigation of mechanical anisotropy of the fused filament fabrication process via customized tool path generation

Carsten Koch, Luke Van Hulle*, Natalie Rudolph

University of Wisconsin-Madison, 1513 University Ave., 53706, Madison, USA

ARTICLE INFO

Article history:
Received 2 February 2017
Received in revised form 9 May 2017
Accepted 14 June 2017

Keywords:
FFF
FDM
Anisotropy
Tool path
Solidity ratio
Orientation
Mechanical
Bead
Properties
SciSlice
Edge effects

ABSTRACT

To aid in the transition of 3D printed parts from prototypes to functional products it is necessary to investigate the mechanical anisotropy induced by the Fused Filament Fabrication (FFF) process. Since the mechanical properties of an FFF part are most greatly affected by the bead orientation and printed density, or solidity ratio, techniques to precisely control these variables are required. An open source Python program, SciSlice, was developed to create the desired tool paths/layer orientations and convert them into machine commands (e.g. G-Code). SciSlice was then used to develop tool paths which either directly printed tensile specimens or printed sheets from which specimens could be water-jet cut. The effects of proper bed leveling and feed wheel adjustment are noted and a careful analysis of both bead orientation and solidity ratio are presented. Printing artifacts related to turns made at the part edges are discussed having been found to have strong effects on the measure strength in the weakest orientation. Finally, it is shown that with proper bead orientation, low layer heights, and a maximum solidity ratio, tensile strengths within 3% of injection molded parts are achievable.

1. Introduction

One of the most common Additive Manufacturing (AM) Material Extrusion (ME) technologies is Fused Filament Fabrication (FFF), commonly referred to by the trademarked name Fused Deposition Modeling™ (FDM™). The process begins to address the challenges of a changing economy and its production requirements. FFF is advancing in its capabilities and material variation and is currently used to manufacture prototypes or small series of specialized parts in various application areas.

FFF is usually compared to injection molding (IM) and in this comparison is often thought to have reduced but unquantified mechanical properties. Therefore, the FFF process needs to be analyzed in detail to understand the contribution of each parameter on the print result. Optimizing the mechanical strength of a printed part may advance the application area of FFF.

High solidity parts with the proper build settings can meet the requirements of increased part reliability and strength. However, the resulting 3D components exhibit extensive anisotropy in their mechanical properties. To better characterize this anisotropy, the focus of this study is on crucial print parameters and their effects on the part's mechanical properties, namely ultimate tensile strength.

The tensile strength of an FFF part in comparison with injection molded parts depends on several parameters, but orientation and solidity of the part are the most significant. This is shown by various studies in the past decades [1–10]. All of these studies have in common that the orientation of the bead was varied and that a bead orientation in load direction (0°) resulted in the strongest FFF parts. The studies also have in common that they were conducted on closed control FFF printers. This means that access to most of the parameters involved in the FFF process are restricted. Complete control over the parameters is not possible using such a system. Closed control in this case means that the print software is supplied with an STL file and the print parameters cannot be chosen independently. In this closed software, the STL file is used to create tool paths which are then translated into proprietary machine commands without the possibility for the user to customize the results at either step. To circumvent these restrictions in research, open source software needs to be developed that allows users the ability to adjust all printing and tool path parameters and a printer needs to be used which accepts an open numeric control language, such as G-code. Fig. 1 exemplifies the different steps using a closed control system (left) and an open source system (right).

Currently the only available FFF printers which use an open numeric control language are the open source or "desktop" FFF

* Corresponding author.
E-mail addresses: koch7@wisc.edu (C. Koch), lvanhulle@wisc.edu (L. Van Hulle), natalie.rudolph@wisc.edu (N. Rudolph).

http://dx.doi.org/10.1016/j.addma.2017.06.003
2214-8604/

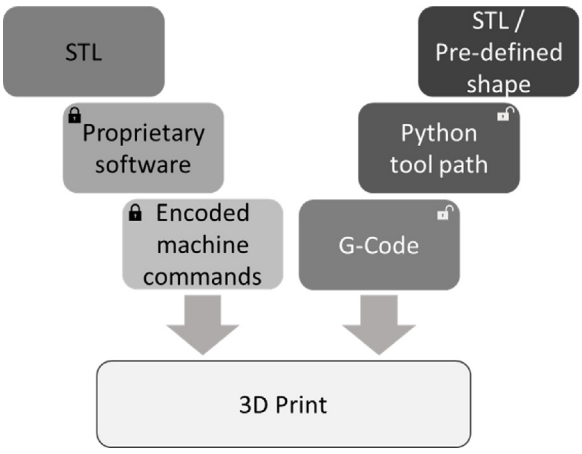

Fig. 1. Different approaches to create a 3D Printed Part.

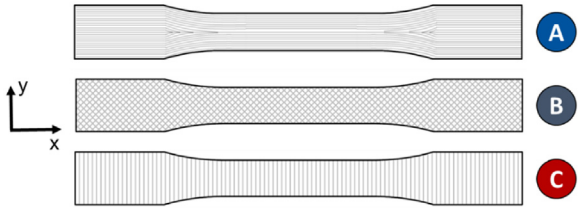

Fig. 2. Different bead orientation within a layer with respect to the X-axis; A: 0°, B: ±45°, C: 90°.

printers, which all use various flavors of G-code. With an open tool path planning program and an open FFF printer full control of the process is enabled allowing the understanding of the interdependencies between parameters in the FFF process. This leads again to the terms orientation and solidity. To optimize the part strength, understanding and controlling solidity is as important as bead orientation. After initial tests with an open source printer, both parameters were defined, which will be explained in the subsequent section.

1.1. Orientation

The term orientation is often used within the FFF process and can be divided into two major fields. The build orientation defines the stacking direction of the 2D layers and the bead orientation refers to the direction of the extruded beads within a layer with respect to the X-axis. Fig. 2 shows the same tensile test specimen printed with three different bead orientations.

Part A is printed in 0° orientation; in line with the X-axis. Part B is printed alternating between +45° and −45° orientation. Part C is printed 90° to the X-axis; in line with the Y-axis. Various studies have proven that beads oriented in load direction (0° orientation) are always stronger than beads oriented perpendicular to the load. The highest values reported reach up to 70 % of the tensile strength of the bulk material determined by testing injection molding (IM) samples of the same material. Deviating from the alignment in load direction, an increasing angle leads to a steady decrease in tensile strength. Parts with beads oriented alternating in +45° and −45° are weaker than in 0°. Parts with an angle deviating more than 45° usually fail along the beads as a result of the forces applied on the weld lines between two beads. The weakest orientation is consequently 90°. In this case, the force is directly applied on the interfaces between two beads. This leads to a failure of the part at the weld line and therefore lower ultimate tensile strength is observed [1–10].

1.2. Solidity

The solidity of an additive manufactured part is crucial for its mechanical properties. Usually, FFF parts are printed with a cross-hatched structure on the inside of the part, or infill, which reduces the weight and build time of a part. However, to achieve stronger parts it is necessary to print in the proper orientation with beads as close together as possible throughout the entire part. This distance is typically the nozzle diameter. These highly dense parts were expected to be stronger than parts with the usual partially filled pattern on the inside. But even a part printed with beads alongside each other can vary in solidity. This solidity is defined by the voids between adjacent beads. The density or solidity defined within this study is called solidity ratio (SR). Fig. 3 shows an illustration of a printed parts' cross section to further explain the term SR as well as its expansion. SR determines the porosity or solidity of the part. The SR is a normalized density where a theoretical minimum is shown by an ellipsoid bead shape ($\frac{\pi}{4}$), which results in large voids between beads (Fig. 3a), up to a fully solid part with the SR of 1.0 and no voids. Fig. 3b shows an increased SR with almost no voids. The SR is calculated by the area of the bead divided by the potential maximum area between the beads, indicated by the box around the bead. This maximum area is bounded by the width of the bead and the layer height. The width of the bead is thereby usually the diameter of the nozzle. By presetting the LH and using a designated nozzle, the SR is controlled by the volume flow. Thus an increase in the volume flow rate of filament increases the SR.

Agarwala et al. [11], Sun et al. [12], and Li et al. [8] conducted research concerning the distance between beads. As beads are layed closer to each other the shape of the bead changes from an ellipsoid to a rectangle. This approach is different than increasing the volume flow rate but the change of the bead shape and thus solidity is comparable. The increasing solidity thus increases the welding area between beads which leads to higher part strength. Conclusively, it can be said that a larger welding area affects the tensile strength posivitevely. However, the effect of a larger welding area generated by an increase in volume flow rate has not yet been examined.

1.3. Edge effects

Producing test specimens with a bead orientation perpendicular to and 45° from the load direction leads to turns or curves on the outside of the part. This can be seen in Fig. 4.

These characteristic curves around the edges, where the printhead moves over to the next adjacent tool path, could affect the tensile strength of an FFF part. This effect has not yet been researched. To achieve a surface without these edges a tool path

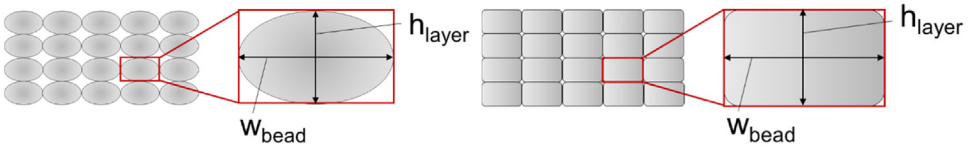

Fig. 3. a (left) and 3b (right): Cross-section of beads with lower (left) and higher (right) SR.

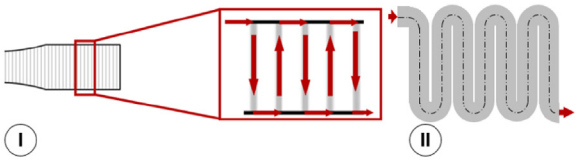

Fig. 4. Schematic of tool path in 90° Orientation (I) and characteristic material curves on the long side of the part (II).

around the part can be added, which is referred to as shell. This shell is printed first in every layer and the rest of the layer is filled using the default orientation. One of the reasons why the effects of these parameters on the tensile strength have not been investigated is that most of the research in this field was conducted using closed control FDM™ machines [1–15].

2. Experimental

2.1. Tool path planning

A custom Python™ program named SciSlice was written to generate the tool paths and convert them into G-Code. SciSlice allows for the customized adjustment of nearly all printing parameters, including infill orientation, in a layer by layer and even region by region basis. Currently available software allows users to adjust many parameters but not infill orientation and not on a per layer basis. Some software allows for straight, hexagonal, or triangular infill, but only provides a default ±45° infill direction. Creative model placement into the slicing software can turn the ±45° into 0°/90° orientations but specimens outside of these two options are not possible. SciSlice can create tool paths at any angle independently for each layer. This enabled the creation of the pure 0° and pure 90° parts used in this study.

To reduce the need for additional files the outline of the ASTM-D638 Type 1 dog-bone test specimen was pre-defined in the program. When generating a tool path the user either loads pre-existing parameters into the program or sets new ones in the user interface after which tool path generation begins.

When a tool path is generated SciSlice first develops an outline for the printed part. If shells are needed additional outlines are created at the specified offset distance inward, with one additional outline created to account for the width of the shell's inner most printed bead. This inner most unprinted outline will be used as a trim line for the infill.

To create the infill a line field is generated with the user specified spacing and orientation. This field is then centered over the trim outline and trimmed appropriately with lines outside the desired print area being removed. The shells and infill are then combined to create a layer. This process is repeated for each layer in the part.

After a layer has been created its lines are sorted into a print order and direction. Currently the sorting algorithm starts at the lowest left endpoint, picks its line, moves to the other end of that line, and then selects the next nearest endpoint. The process of moving to the line's opposite end and then choosing the next nearest endpoint is repeated until every line has been selected.

Next the sorted layer is converted into a tool path by applying all the additional non-printing moves plus pre/post layer extrude/retract requirements to help prevent nozzle drool. Finally, the tool path is translated into G-Code and written to a text file. SciSlice is available open-source [16].

2.2. Material

All print experiments were conducted with commercially available acrylonitrile butadiene styrene (ABS) manufactured by MatterHackers Inc. The filament is 2.93 mm in diameter with an estimated accuracy of ±0.07 mm provided by the manufacturer. The recommended extrusion temperature range is 230–250 °C and the recommended print-platform temperature is 110 °C. The material ABS was chosen because of its common use in FFF printing, its good mechanical properties regarding stiffness, and its high dimensional stability. The density is given as 1.07 g/cm^3. The material was ordered in its natural color to eliminate influences of color pigments and additives.

2.3. Sample preparation

The FFF printer used for all tests is a LulzBot™ TAZ 5. The hot end of the printer was heated to 250 °C and the print platform to 110 °C. All of the test specimens were printed with an XY travel speed of 2000 mm/min. The bead orientation is varied between 0°, ±45° and 90° in respect to the load direction of the test specimen, Fig. 2. The solidity ratio is varied between 0.9 and 1 since the goal is to produce the strongest parts possible. The SR of the 90° oriented specimens was varied between 0.6 and 1 to investigate the influence of the solidity ratio on the tensile strength for the supposedly weakest orientation. The start of every layer is set to the lower left corner of the dog-bone and kept constant.

To produce an accurate SR the volumetric flow rate of the incoming filament needs to be known. However, since FFF printers control extrusion by linear feed of filament and there are fluctuations in volume per unit length of filament caused by changes in diameter of and voids within the filament, volumetric flow rate cannot be precisely controlled. To compensate these fluctuations in SR, the solidity ratio of every specimen was corrected. This correction was made by dividing the volume of the printed specimen, defined by the weight of the specimen and the density of the material, by the G-Code volume, the prescribed filament area times the length of filament extruded.

The edge effects, and more particularly the stress concentrators at the notches between turns, were researched using three different approaches.

First, a large sheet with the orientation of 90° was printed using the same parameters as the other prints. Then, dog-bone test specimens were cut out of the sheet using a water-jet cutter (WJC). This technique was used to produce specimens in both 0° and 90° orientations.

Second, two shells were added around the 90° oriented dog-bones. The width of the infill oriented in 90° was corrected to maintain the dimensions of the test specimen. These two shells, adding up to 1 mm in width, around every layer of the test specimen were analyzed concerning their impact on part strength. Supporting the structure with 1 mm of bead in load direction and eliminating the notched edges on the surface of the part are assumed to lead to a better stress distribution and increased part strength.

Third, the edges were smoothed using acetone vapor. This process enables a reliable and reproducible smooth surface on the specimen. The specimens were exposed to the acetone vapor in a glass chamber. An initial group of specimens were placed in the chamber between 0.5 and 3 h. No additional smoothing was observed after the 2 h mark leading to that time being used for further vapor smooth samples. The parts were not tensile tested for at least 96 h to allow full diffusion and evaporation of the acetone.

To compare the results with injection molded parts, the same ABS material that was used for the FFF parts was pelletized in a Scheer SGS 100-E pelletizer. These pellets were transferred to a Boy XS injection molding machine to produce Type 5 tensile specimens.

More information about the process settings can be found in Supplementary Materials.

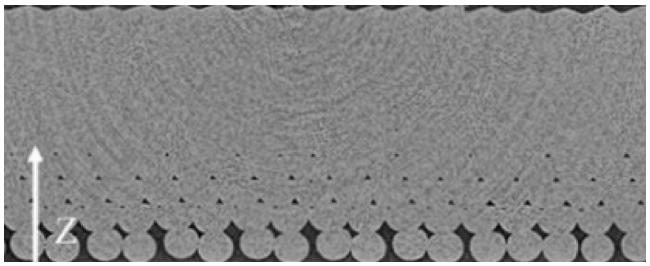

Fig. 5. Cross-section of a specimen printed on an insufficiently leveled bed.

2.4. Testing

Currently no standard is defined to test additive manufactured materials using a tensile test machine. Therefore, ASTM D638-14 "Standard Test Method for Tensile Properties of Plastics" was used and the preferred Type 1 tension test specimen with a gauge section width of 13 mm was used to determine the mechanical properties of the printed materials, while the smaller Type 5 specimen with a gauge width of 3.18 mm was used for the injection molded parts [17].

The tensile tests were performed with an Instron 5967 Dual Column Tabletop Model testing system with a load cell of 30 kN and a test speed of 5 mm/min.

After vapor smoothing and before tensile testing the surface roughness and radii of the notches were measured with an Alicona InfiniteFocus micro coordinate measurement device.

3. Results

3.1. Printer setup

Preliminary tests were executed to evaluate proper settings for the FFF printer. General tests regarding the determination of nozzle temperature and extrusion speed were explained by Pfeifer et al. [18]. In addition, the effect of bed leveling on the part properties was investigated. It was shown that proper bed-leveling is crucial for good adhesion of the part to the print bed, but also to achieve the desired layer height for the first layer. Fig. 5 shows the cross section from a μCT scan of a printed test specimen with insufficient bed-leveling.

In this case the print-bed is too low which significantly affects the first layer. The first beads are laid down without the required Z-height constriction to form them into an ellipsoid shape. This error has two effects. First, the surface-area of the bead and therefore the contact area to the print-platform is smaller than expected. This reduced surface-area leads to reduced bed adhesion. Second, the density of the part decreases because of the large voids within the first layer and the smaller voids between the first and second layer. Not every bead touches all of its adjacent neighbors as is desired in these tests. This configuration means that the theoretical SR is not achieved and the parts exhibit a through thickness density gradient.

In a second test, the effect of the contact pressure of the feeding gear on the filament was investigated. If the pressure is too low the gear starts to slip and grinds down the filament. This assertion is verifiable by the small slivers of filament that can be found on the inside of the feeding system. The force can be adjusted by tightening two screws on the contact pressure wheel assembly. Too much contact pressure might result in crushing the filament at the point where the wheel touches the filament. This crushing reduces the distance between the feeding gear and the contact pressure wheel. The smaller distance inhibits incoming material, with the original diameter, from entering the feeding system. Consequently, the material is ground down at that point and no more material is fed into the nozzle.

Therefore, it is important to test if the right contact pressure is applied. This is done by using a G-Code program which commands a specified length of filament be extruded. This filament needs to be weighed and then compared to the weight of the extruded material. The difference in weight accounts for the extrusion error due to insufficient contact pressure. The impact of deficient contact pressure is shown in Fig. 6. Fig. 6 shows two sets of five specimens. For each set the parts were printed one after another without pausing the print. One of the sets was printed without properly adjusting the feeding system and the samples show a large variance within the series. The insufficient contact pressure on the filament leads to slippage of the filament and therefore to under-extrusion. After correcting the contact pressure, the feeding system works reliably and all specimens have a similar SR.

3.2. Effect of bead orientation

Bead orientation was confirmed to have a great influence on the tensile strength of FFF parts. Fig. 7 displays the results for three orientations compared to an injection molded (IM) part using a layer height of 0.2 mm and a SR between 0.95 and 0.97.

The injection molded test specimens reached a tensile strength of 41 MPa, close to the FFF parts printed in 0° orientation. The parts

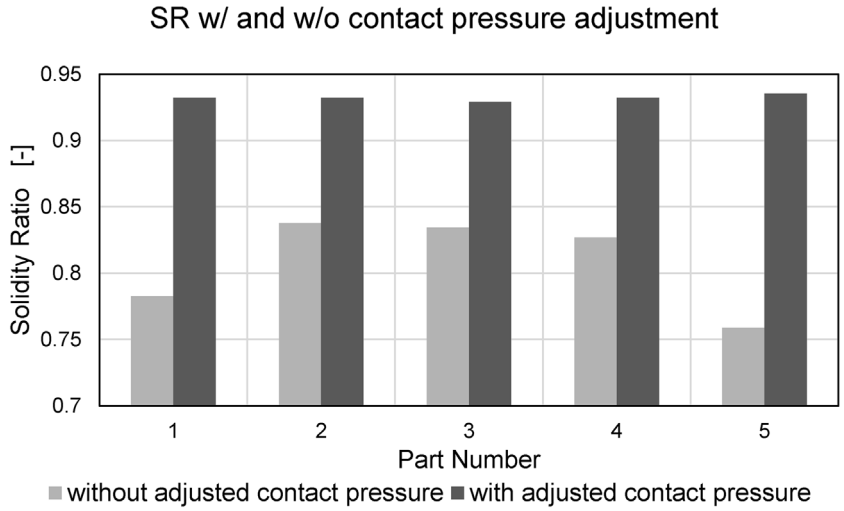

Fig. 6. Variability of SR within test series with and without properly adjusted contact pressure.

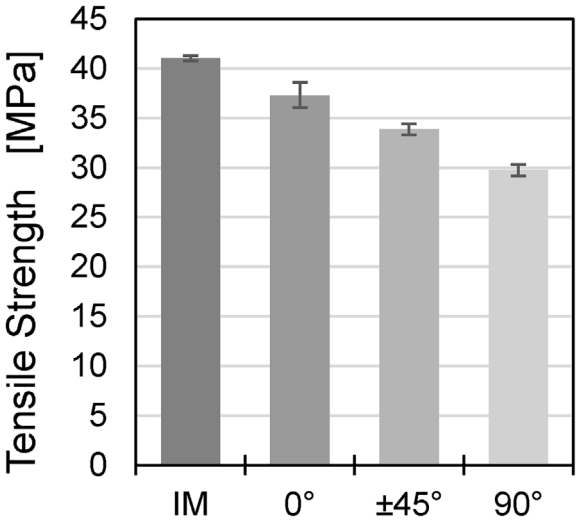

Fig. 7. Tensile strength of different print orientations (Layer height 0.2 mm and SR of 0.95-0.97) compared to IM parts.

printed in load direction with solidity ratio of 0.96 achieve 92.3% of the strength of an injection molded part. By increasing the SR to 0.99, the tensile strength can be increased to 97% of an IM part. The parts with an alternating orientation of ±45° reach a tensile strength of 33.8 MPa.

The weakest parts were printed with beads perpendicular to the load direction and had a tensile strength of 29.75 MPa. Even though this is the lowest tensile strength, it still reaches 72% of the strength of an IM part. In all cases the elongation at break of an FFF part is 20 times lower than injection molded samples.

These results show the anisotropy in FFF parts is consistent with the studies mentioned in Section 1.1. However, most of the earlier studies resulted in maximum tensile strengths around 70% when using a bead orientation in load direction. Our study exceeds this strength even in the 90° orientation when highly-customized print settings are used and high solidities are achieved.

3.3. Effect of solidity ratio

The effect of a change in solidity ratio was researched using all three orientations. In this paper the effect of SR on 90° oriented beads is discussed. To investigate the effect of a lower SR the test range was expanded to SR from 0.63 to 1.0. All parts were printed with a layer height of 0.3 mm. The results are displayed in Fig. 8.

The tensile strength of the parts with a SR of 0.63 and 0.64 is almost equal. These two SR are lower than $\frac{\pi}{4}$ which is the minimum SR where every bead touches its adjacent neighbors. This means that beads of different print-layers are stacked on top of each other without touching the beads adjacent to them within their layer. This leads to the assumption that the load is carried primarily by the corners where the print-head turns around to print the next bead. Increasing the SR over the threshold of $\frac{\pi}{4}$ leads to a steady increase in tensile strength. Whereas the lowest SR reaches a tensile strength of only 3.4 MPa the highest SR reaches a value of 28.65 MPa. That means the highest SR in 90° orientation reaches 69.86% of the strength of an IM part and 77.4% of a printed part with the same SR and a 0° orientation. The elongation of parts with a SR up to 0.97 is between 2 and 4% and therefore lower than for the parts in 0° orientation and just 2% of an IM part. However, increasing the SR to 100% leads to a larger elongation of up to 7% which is more than in specimens printed in load direction.

The same effects occurred in every orientation but are stronger if the beads are oriented perpendicular to the load direction. Due to the fact that the failure of 90° oriented parts occur at the bead weld lines, the effect of an increase in SR is higher than for other orientations.

3.4. Edge effects

The different techniques to eliminate the notches on the part surface (vapor smoothing, water-jet cutting (WJC), and adding shells) and the resulting tensile strength are shown in Fig. 9. The sheet printed for the WJC had a LH of 0.2 mm and a SR of 0.95. The smoothed specimens and the specimens with two shells were also printed with a LH of 0.2 mm and a SR of 0.96 and 0.97 was reached, respectively.

Samples cut with the water-jet cutter exhibit the lowest tensile strength of 13 MPa. The samples with a 1 mm shell added are the strongest (31.3 MPa) and slightly stronger than a regular 90° dog-bone (29.75 MPa). The smoothed sample was kept in acetone vapor for 2 h and the tensile strength of 26.03 MPa is weaker than non-smoothed test specimens. All the different test specimens elongate up to 2% at break. However, the elongation increases with a larger SR in the same way it does for regular 90° oriented test specimen.

The edge effects were eliminated by using a water-jet cutter to remove the extra edge material created at each turn of the print head. This edge effect has a significant influence on the tensile strength of the part and removing the corners leads to significantly weaker parts. The reduction of over 56% compared to regular 90° test specimens shows the great influence of these corners on tensile strength.

Adding 1 mm of shell around the part does not change the strong effect of the edges on the tensile strength. The added shells provide a smoother surface of the part and make the part slightly stronger since 2 mm of the width of the specimen are now aligned with the load direction. Conclusively, adding shells around the part improves the surface quality as well as the strength of the part.

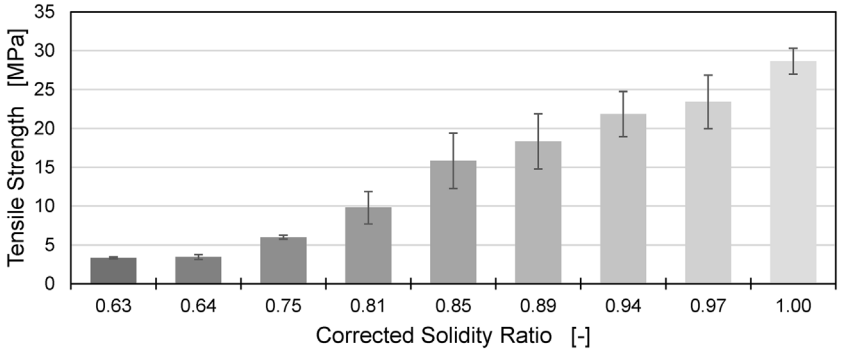

Fig. 8. Tensile strength of 90° oriented tensile specimens with 0.3 mm LH as a function of SR.

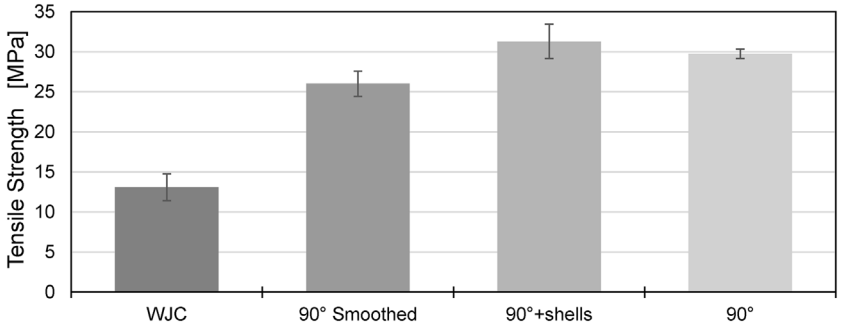

Fig. 9. Tensile strength of different post-processing techniques (0.2 mm LH and SR of 0.96–0.97).

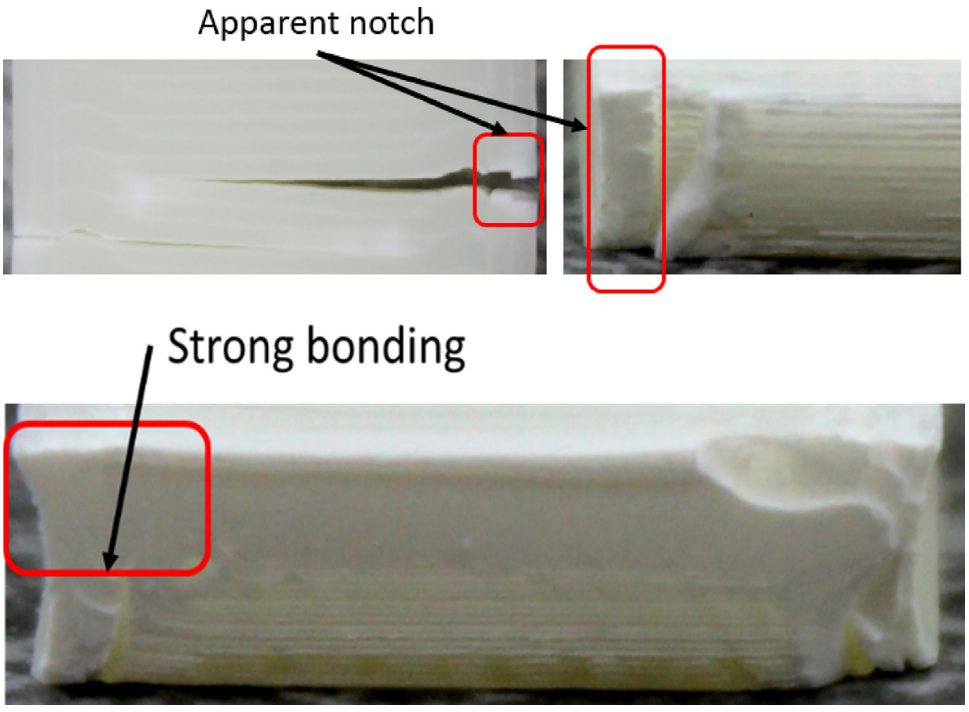

Fig. 10. a (top): Imperfect bonding between shell and infill using a SR of 0.95; 10a left: Top view of specimen. Load direction is out the top and bottom of picture. 10a right: Front view of break. Shells are on left, load direction is in and out of page. b (bottom): Strong bonding between shell and infill using a SR of 1. Front view of break. Shells on left and right side, load direction in and out of page.

Fig. 10a and b shows that the welding between the shell and the infill is dependent on the SR of the specimen. Fig. 10a shows the top and front view of two tensile specimens with a SR of 0.95. Both parts show a visible weld line and notch between the shell and the infill.

A test specimen with a SR of 1 shows strong bonding between the shell and the infill so that the weld line cannot be seen in the fracture surface of the tested specimen (Fig. 10b).

Even though a difference between the two SR is apparent, the part always fails perpendicular to the load direction and along the weld line of the infill. This failure occurs at the same location in the shell and the infill indicating that the bonding strength is strong enough to avoid delamination between the shell and the infill.

Acetone vapor smoothing increased the surface quality of the dog-bones. Fig. 11 shows the edges of a specimen before and after the smoothing.

The typical edges on the side of the part (left picture) as well as the bead structure on top of the part almost disappeared after 2 h in the smoothing device (see right picture). The process improves the visual quality of the part but negatively effects its strength. It was observed that the parts were softer when they were removed from the device. This leads to the assumption that the negative effects of the acetone on the tensile strength of the part as a whole were greater than the reduction of stress concentrators at the turns.

3.5. Conclusions

This study is focused on the research of highly dense parts achieved by printing with a high SR. This approach helps to understand the correlation between different print parameters and is an attempt to explain different phenomena in FFF manufacturing. However, commonly used print settings of FFF machines create a less dense part by using an infill pattern that creates hollow sections within the part. This strategy is used to significantly reduce part weight and built time but greatly sacrifices tensile strength. The results show that parts with a high SR and low layer heights reach the tensile strengths in line with IM parts. The parts with a lower SR, similar to parts printed with sparse infill, show a lower tensile strength.

Even though highly dense parts achieve strengths in line with IM parts, this is not the way FFF parts are usually produced. This discrepancy can be explained by focusing on the major advantages of the FFF process. The freedom of design, faster development, lighter structure, and reduced short run costs are the major benefits of

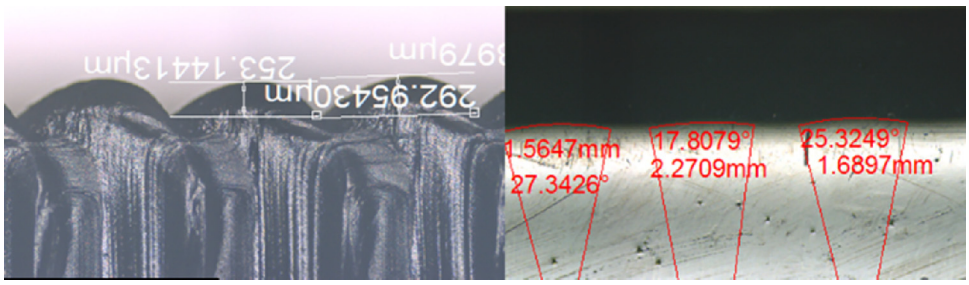

Fig. 11. Side of a test specimen with corners (left) and after smoothing (right).

this process. Therefore, the goal of FFF is not to compete with the strength or high production speed of injection molding but instead the goal is to expand the capabilities of plastics processing in general.

This perception, however, does not preclude the need for a comparison of parts concerning mechanical strength. One approach used in the field of fiber reinforced plastics is the plotting of tensile strength as a function of the specific density of a material. In this way, a material independent strength can be shown by dividing tensile strength with the specific density [19]. A similar approach could also be used for FFF parts.

In this study the solidity ratio of the printed beads is defined and researched. Instead of using the SR of a single bead, the SR of a part could be calculated. Therefore, the volume of the part needs to be taken into account. Producing a part via IM leads to a fully filled volume of the part. In FFF however, a hollow infill structure can be used to decrease the density of the part. The weight divided by the density would then result in a SR for the part. Therefore, the tensile strength of the specimen could be divided by the SR of the part leading to a specific strength of the specimen. This specific strength could be plotted over the SR of the part. This method would normalize the mechanical strength of the part and may lead to a comparability of FFF depending on its inner structure. The results show that a part printed with a bead orientation in the load direction combined with a small LH and high SR almost reaches the strength of an IM part. Normalizing this strength with the introduced method leads to a tensile strength of 40.26 MPa for a SR of 0.97 and a LH of 0.1 mm. This is 98% of the strength of an IM part. However, this approach is less accurate for lower SR. The smaller the SR of the part the higher the divergence between the specific strength of an FFF part and the strength of an IM part even with normalization. This indicates that the correlation between tensile strength and SR is not linear.

Similar observations were made for an orientation perpendicular to the load direction. Parts with low SR are much weaker than an IM part, and even high solidity parts do not reach 75% of the strength of an IM part. Importantly, the SR effect in the 90° orientation is stronger than in 0°. Therefore, the effect of the SR on the weld line behavior and the effects of larger voids in low SR parts needs to be analyzed. In addition, orienting beads at 90° results in the typical notched surface, which also affects the strength of a part. The whole approach shows that SR affects part strength in a non-linear way and that further investigations need to be conducted to calculate the exact influence. Once this is achieved, the tensile strength of parts with different SR can be normalized and compared to each other as well as to injection molded specimens.

4. Outlook

The study confirmed the effect of bead orientation on tensile strength. It was further shown that the solidity ratio and the weld area have an effect on the strength. Therefore, the presented approach is currently being extended to compressive and flexural tests and analysis methods to assess the weld strength are being investigated. One approach applies composite laminate theory on the results to test the specific strength hypothesis and its applicability to FFF parts. The observed reinforcement of the parts due to the turns around the part edges will be investigated further and related to the layer print time as well as a print times between turns. This study is currently expanded by measurements of the temperature field during printing to test this relation.

The reduced elongation at break is also thought to be related to the weld strength between beads. Future work will aim at understanding the failure mechanisms at the interface and their relation to part brittleness.

The current results as well as the on-going studies will be used to inform tool path planning. By combining FEA analysis with the tool path planning software beads could be prioritized during sorting to reduce cooling times in high stress areas. The ability to produce custom layer orientations in different subsections of a layer combined with topology optimization and anisotropic parameters will allow for producing parts with enhanced bead alignments increasing a part's strength to weight ratio over generic ±45° prints. By knowing which regions of a layer are in tension and which are in compression parts could be printed with larger layer heights in compressive areas significantly reducing print times without major effects on part strength.

Appendix A. Supplementary data

Supplementary data associated with this article can be found, in the online version, at http://dx.doi.org/10.1016/j.addma.2017.06.003.

References

[1] S.-H. Ahn, M. Montero, D. Odell, S. Roundy, P.K. Wright, Anisotropic material properties of fused deposition modeling ABS, Rapid Prototyp. J. 8 (4) (2002) 248–257.
[2] O.S. Es-Said, J. Foyos, R. Noorani, M. Mendelson, R. Marloth, B.A. Pregger, Materials and manufacturing processes effect of layer orientation on mechanical properties of rapid prototyped samples effect of layer orientation on mechanical properties of rapid prototyped samples, Mater. Manuf. Process. 15 (1) (2000) 107–122.
[3] K. Kirchner, H. Jäschke, H.-J. Franke, T. Vietor, K.-H. Grote, Mechanisch-technologische Eigenschaften generativ gefertigter Bauteile in Abhängigkeit von der Bauteilorientierung, RTejournal (2010) 1–8.
[4] M. Montero, S. Roundy, D. Odell, Material characterization of fused deposition modeling (FDM) ABS by designed experiments, Proc. Rapid Prototyp. Manuf. Conf (2001) 1–21.
[5] A.K. Sood, R.K. Ohdar, S.S. Mahapatra, Improving dimensional accuracy of Fused Deposition Modelling processed part using grey Taguchi method, Mater. Des. 30 (1) (2009) 4243–4252.
[6] I. Durgun, R. Ertan, Experimental investigation of FDM process for improvement of mechanical properties and production cost, Rapid Prototyp. J. 20 (3) (2014) 228–235.
[7] A.M. Kloke, Untersuchung der Werkstoff-, Prozess- und Bauteileigenschaften beim Fused Deposition Modeling Verfahren, Universität Paderborn, Paderborn, 2016.
[8] L. Li, Q. Sun, C. Bellehumeur, P. Gu, Composite modeling and analysis for fabrication of FDM prototypes with locally controlled properties, J. Manuf. Process. 4 (2) (2002) 129–141.

[9] J.F. Rodríguez, J.P. Thomas, J.E. Renaud, Mechanical behavior of acrylonitrile butadiene styrene fused deposition materials modeling, Rapid Prototyp. J. 7 (3) (2001) 148–158.
[10] J.C. Riddick, M.A. Haile, R. Von Wahlde, D.P. Cole, O. Bamiduro, T.E. Johnson, Fractographic analysis of tensile failure of acrylonitrile-butadiene-styrene fabricated by fused deposition modeling, Addit. Manuf. 11 (2016) 49–59.
[11] M.K. Agarwala, V.R. Jamalabad, N.A. Langrana, A. Safari, P.J. Whalen, S.C. Danforth, Structural quality of parts processed by fused deposition, Rapid Prototyp. J. 2 (4) (1996) 4–19.
[12] Q. Sun, G.M. Rizvi, C.T. Bellehumeur, P. Gu, Effect of processing conditions on the bonding quality of FDM polymer filaments, Rapid Prototyp. J. 14 (2) (2008) 72–80.
[13] D.P.B.S.J. Riddick, J.C. Hall, A.J. Haile, M.A. Wahlde, R.V. Cole, Effect of manufacturing parameters on failure in Acrylonitrile–Butadiane–Styrene fabricated by fused deposition modeling, Struct. Dyn. Mater. Conf. vol. 53 (2012) 1–8, April.
[14] A. Bellini, S. Güçeri, Mechanical characterization of parts fabricated using fused deposition modeling, Rapid Prototyp. J. 9 (4) (2003) 252–264.
[15] M. Bertoldi, M. a Yardimci, C.M. Pistor, S.I. Guceri, G. Sala, Mechanical characterization of parts processed via fused deposition, Solid Free. Fabr. Proc. (1998) 557–565.
[16] L. Van Hulle, SciSlice, 2016. [Online]. Available: http://pec.engr.wisc.edu/facilities_AM.html.
[17] N.N., ASTM D638-14 Standard Test Method for Tensile Properties of Plastics, ASTM, International, West Conshohocken, PA, 2014.
[18] T. Pfeifer, C. Koch, L. Van Hulle, G.A. Mazzei Capote, N. Rudolph, Optimization of the FDM additive manufacturing process, in: Proceedings of the Annual Technical Conference (ANTEC) of the Society of Plastics Engineers, Indianapolis, 2016, pp. 22–29.
[19] G. Menges, E. Haberstroh, W. Michaeli, E. Schmachtenberg, Menges Werkstoffkunde Kunststoffe, Carl Hanser Verlag GmbH & Co KG, München, 2011.